Polymer Chemistry

Accepted Manuscript

This is an *Accepted Manuscript*, which has been through the Royal Society of Chemistry peer review process and has been accepted for publication.

Accepted Manuscripts are published online shortly after acceptance, before technical editing, formatting and proof reading. Using this free service, authors can make their results available to the community, in citable form, before we publish the edited article. We will replace this *Accepted Manuscript* with the edited and formatted *Advance Article* as soon as it is available.

You can find more information about *Accepted Manuscripts* in the Information for Authors.

Please note that technical editing may introduce minor changes to the text and/or graphics, which may alter content. The journal's standard Terms & Conditions and the Ethical guidelines still apply. In no event shall the Royal Society of Chemistry be held responsible for any errors or omissions in this *Accepted Manuscript* or any consequences arising from the use of any information it contains.

ROYAL SOCIETY OF CHEMISTRY

www.rsc.org/polymers

Journal Name

ARTICLE

The synthesis, characterization and flexible OFET application of three (*Z*)-1,2-bis(4-(tert-butyl)phenyl)ethane based copolymers

Received 00th January 20xx,
Accepted 00th January 20xx

DOI: 10.1039/x0xx00000x

www.rsc.org/

Yuli Huang, Wei Huang, Junwei Yang, Ji Ma, Moyun Chen, Haoyun Zhu and Weizhi Wang*

We report herein three *(Z)*-1,2-bis(4-(tert-butyl)phenyl)ethane based alternating copolymers synthesized with thiophene (**PBPT**), thieno[3,2-b]thiophene (**PBPTT**) and dithieno[3,2-b:2',3'-d]thiophene (**PBPDT**) moieties. Their optical characteristics, morphology, orientation, and application in the flexible organic field effect transistor (OFET) devices were studied in this research. Copolymer **PBPTT** shows interesting properties, such as, the almost planar molecular structure with the extended π-conjugation degree, the ordered edge-on orientation in a fiber-like film, and the thieno [3,2-b] thiophene moiety located in the middle of the polymer backbone for its symmetric and strong π-stacking effect. Moreover, **PBPTT** was successfully used to fabricate ambient stable and high performance, flexible OFET devices, with charge carrier mobility up to 0.27 $cm^2V^{-1}s^{-1}$ and on/off ratio = 10^4. The study reveals the profound influence of the fused thiophene and symmetric molecular structure on the copolymer characteristics and OFET device performance， and offers us a novel strategy to design semiconductor polymers for OFET application.

Introduction

Conjugated polymers have been deeply studied for use in organic field effect transistors (OFETs) because their advantages, such as cost-effective, large-scale solution process,[1-5] and potential application in the electronic industry.[6-10] Recently, the progresses in organic dielectric layers[11, 12] and polymer substrates fuel the research of flexible OFET devices.[13-15] Especially, the OFETs with ion gel dielectric show high charge carrier mobility and low operating voltage, which are promising candidates for flexible devices in the future.[16-25]

For OFETs, the planar main chain structure has been proven one of the crucial factors to increase the charge mobility.[26-29] Thiophene moiety has been known to be an excellent building block for semi-conductive polymers and small molecules,[30] because it is electron rich and promotes intermolecular π-π stacking. For example, regioregular poly(3-hexythiophene) (P3HT) which is one of the most widely used semi-conductive polymers exhibits charge carrier mobility up to 0.1-0.4 $cm^2V^{-1}s^{-1}$.[31, 32] Furthermore, the fused thiophene has been shown to increase coplanarity along the backbone and π-π stacking in solid state more effectively, which is greatly beneficial for charge transport properties.[29, 33-39]

In our research, the thiophene and fused thiophene moieties are copolymerized with the *(Z)*-1,2-bis(4-(tert-butyl)phenyl)ethane moiety synthesized by ourselves.[40] The synthetic process (Scheme S1†) and characterization data (Table S1† and Fig. S1-5†) are shown in the supporting information. We want to combine the great semi-conductive properties of thiophene and fused thiophene with the locating effect coming from the cis configuration of the comonomers made by ourselves, to produce a series of copolymers with the conformation that thiophene and fused thiophene moieties are in the middle of the backbone， as shown in Scheme 1. In addition, the tert-butyl side-chains of bis(4-(tert-butyl)phenyl)ethane have the ability to improve the solution processability of copolymers with large conjugated structure. These copolymers are hoped to own ordered conformation and aggregation structure to give an excellent semiconductor performance.

In this paper, we report the synthesis of three polymers by copolymerization of *(Z)*-1,2-bis(4-(tert-butyl)phenyl)ethane moiety with thiophene, thieno[3,2-b]thiophene, dithieno[3,2-b:2',3'-d]thiophene. Then the solution UV-vis absorption and PL emission spectra were utilized to study the molecular conformation of the copolymers. The orientation of the copolymer films was probed by two-dimensional grazing-incidence X-ray diffraction. The atomic force microscope and polarizing microscope were used to observe the morphology of the copolymers. Finally, the flexible OFET devices were fabricated to research the semi-conductive properties of these copolymers.

[a] *State Key Laboratory of Molecular Engineering of Polymers, Department of Macromolecular Science, Collaborative Innovation Center of Polymers and Polymer Composite Materials, Fudan University, Shanghai 200433, P. R. China. E-mail: weizhiwang@fudan.edu.cn.*

†Electronic Supplementary Information (ESI) available: MALDI-TOF data, crystal data, GPC data，^{1}H-NMR and ^{13}C-NMR spectra， TGA and DSC Curves， Cyclic voltammograms，POM photos，AFM photos，output curves and linear fitting information and OFET performance table for ambient stability. See DOI: 10.1039/x0xx00000x

Experimental Section

Materials. Unless otherwise stated, all reagents and chemicals used were purchased from Aldrich, J&K and Sinopharm Chemical Reagent Company. Toluene was distilled with sodium wires and benzophenone, added under nitrogen (N_2) immediately prior to use. The 2,5-diiodothiophene was purchased from TCI. The 2,5-dibromothieno[3,2-b]thiophene was purchased from J&K. The 2,6-dibromodithieno[3,2-b:2',3'-d]thiophene was purchased from Aldrich.

Measurement and Characterization.

Polymer molecular weights were analyzed by Agilent/Wyatt 1260 Gel permeation chromatography (GPC) system with THF as an eluent against polystyrene as standards. The NMR spectra were recorded at room temperature using a Bruker AVANCE III HD 400 MHz FT-NMR NMR spectrometer in deuterated dichloromethane (CD_2Cl_2). Chemical shifts (ppm) were reported with tetramethylsilane as an internal standard. Absorption spectra were recorded using a Perkin-Elmer Lambda 750 UV-visible Spectrophotometer as a solution in chloroform (10^{-5} M). Photoluminescence spectra (PL) were performed in chloroform solvent (10^{-5} M) on a Photo Technology International, Inc. QM40 fluorescence lifetime spectrometers at room temperature. Cyclic voltammetric measurements (CV) were performed on a CHI 600E electrochemical workstation with a three-electrode cell in a solution of 0.1 M tetrabutylammonium hexafluorophosphate ($TBAPF_6$) in acetonitrile at room temperature with a scan rate of 50 mV/s. A platinum wire, a glassy carbon electrode and an $Ag/AgNO_3$ electrode were used as the counter electrode, working electrode and reference electrode, respectively. The polymer film was coated on the working electrode by using a polymer solution in chloroform and dried in air for 10 min. The HOMO levels were derived from the equations: $E_{HOMO} = -(E_{onset\text{-}ox}\text{-}0.0468+4.8)$ (eV), where $E_{onset\text{-}ox}$ is the onset oxidation potential determined from cyclic voltammetry for oxidation potentials and the value 0.0468 V is for FOC vs Ag/Ag^+. The LUMO levels were derived from the band gap and HUMO levels by the equation: $E_{LUMO} = E_g + E_{HOMO}$. Synchrotron-based two-dimensional gazing-incidence X-ray diffraction data (2D GIXRD) were recorded at BL14B1, Shanghai Synchrotron Radiation Facility, with the gazing-incidence angle = 0.25 °and λ = 0.124 nm. Samples were spin-coated on substrates at 3000 r/m for 60s from 0.1 wt % chloroform solution of the copolymers. The thickness of the films was measured by film thickness gauge FILMETRICS F40. Polarizing microscope (POM) Leica DM2500P was employed to observe the morphology of the copolymer. The samples were precipitated by slow volatilization of chloroform solvent in spindly grass tubes. The morphology of polymer films was observed by Bruker multimode 8 atomic force microscopy (AFM). Differential scanning calorimetry (DSC) was carried out on a TA Q2000 differential scanning calorimeter with one heat-cool cycle from 0 °C to 300 °C at a rate of 10 °C/min under a constant N_2 flow. Thermogravimetric analysis (TGA) was done on a Perkin Elmer Pyris 1 thermo gravimetric analyzer with a warming rate of 10 °C/min, under dry N_2 flow.

OFET device Fabrication and Characterization.

Commercially available PET film (2mm) was divided into 3×3cm sheets, then washed with methanol and deionized water in an ultrasonic cleaner for 10min each. The copolymers in chloroform solution (0.1 wt %) were spin-coated on these clean PET sheets at the rotating speed of 6000 r/min. The 100nm thick gold source and drain electrodes (the typical channel length and width are 400 and 1000 μm) were deposited by vacuum evaporation on the copolymer thin film through a shadow mask. A kind of ion gel, which is the mixture of a triblock co-oligomer (PS-PMMA-PS), poly(styrene-block-methyl methacrylate-block-styrene) (M_{PS} =4.3 kg mol^{-1}, M_{PMMA} = 12.5 kg mol^{-1}, M_W = 21.1 kg mol^{-1}), and an ionic liquid (1-ethyl-3-methylimidazoliumbis(trifluoromethylsulfonyl)imide) in ethyl propionate solution, was used as the dielectric layer. The weight ratio of the solvent, ionic liquid and the oligomer was maintained at 15:10:0.7. The prepared ionic solution was drop-casted to cover the surfaces of the drain, source electrodes and copolymer films. Then thin Al foils (thickness of 0.03 mm) were covered on the transistor channels to form the top-gate electrodes. OFET electrical characteristics were measured using Keithley 4200-SCS/F at room temperature in air. The charge carrier mobility and threshold voltage were calculated in the saturation regime using gradual channel approximation equation:[41, 42]

$$I_{DS} = (\mu W C_i/2L)(V_G - V_{TH})^2$$

I_{DS} is the current through the drain and source electrodes. μ is the mobility of charge carriers. C_i is the capacitance per unit area of the gate dielectric layer, which is 10 μF/cm^2 for the ion gel dielectric layer in this research.[16, 17, 23] W and L are the channel width and length of the device. V_G is the gate voltage. V_{TH} is the threshold voltage.

Synthesis of poly((*Z*)-1,2-bis(tert-butyl)phenyl)-thiophene) (PBPT).

A 100 ml round-bottomed flask equipped with a magnetic stir bar was charged with 50 mL dry toluene, 2 M K_2CO_3 (10 mL H_2O), *(Z)*-1,2-bis(4-tert-butyl(phenyl))-1,2-bis(4,4,5,5-teramenthyl-1,3,2-dioxaborolan-2-yl)ethane (1.089 g, 2 mmol), 2,5-diiodothiophene (0.672 g, 2 mmol) and a catalytic amount of tetrakis(triphenylphosphine)palladium ($Pd(PPh_3)_4$) (1.0 mol %) under argon atmosphere. The reaction was at 95 °C for 5 days avoiding light. After cooling to room temperature, the solution was extracted with toluene and concentrated on a rotavap, a black solid was obtained. Then the residue was dissolved in a minimum amount of chloroform and then added dropwisely into methanol. The precipitate was collected by filtration and washed by Soxhlet extraction with acetone to remove remaining unreacted monomers and catalyst. Then the residue solid was dried under vacuum for 1 day to give a brown powder. (0.33 g, 44.3 %). ^{1}H NMR (400 MHz, CD_2Cl_2) δ: 7.29 – 5.90 (m, 10H), 1.34 – 0.97 (m, 18H); ^{13}C NMR (100 MHz, CD_2Cl_2) δ: 149.74, 138.93, 130.33, 128.59, 125.34, 34.45, 30.93, 24.56. $C_{26}H_{28}S$ (372.57): C, 83.82; H, 7.58; S, 8.61. Found: C, 83.20; H, 8.13; S, 8.67 %.

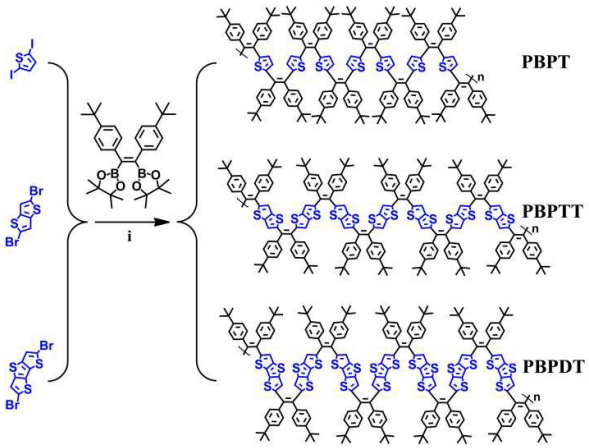

Scheme 1 Synthesis of **PBPT**, **PBPTT** and **PBPDT**. (i) $Pd(PPh_3)_4/K_2CO_3$, toluene/H2O, 95 °C/5 days.

Synthesis of poly((Z)-1,2-bis(4-(tert-butyl)phenyl)-thieno[3,2-b]thiophene) (PBPTT).

Using a procedure similar to that described above for **PBPT**, *(Z)*-1,2-bis(4-tert-butyl(phenyl))-1,2-bis(4,4,5,5-teramenthyl-1,3,2-dioxaborolan-2-yl)ethane (1.089 g, 2 mmol) and 2,5-dibromothieno[3,2-b]thiophene (0.596 g, 2 mmol) were polymerized to give **PBPTT**. The final copolymer is a dark red powder. Yield: 0.569 g (66.1 %). ^{1}H NMR (400 MHz, CD_2Cl_2) δ: 7.24 – 6.30 (m, 10H), 1.48 – 0.88 (m, 18H); ^{13}C NMR (100 MHz, CD_2Cl_2) δ: 150.09, 147.43, 139.47, 130.56, 124.40,121.61 34.31, 29.67. $C_{28}H_{28}S_2$ (428.65): C, 78.46; H, 6.58; S, 14.96. Found: C, 78.33; H, 6.96; S, 14.71 %

Synthesis of poly((Z)-1,2-bis(4-(tert-butyl)phenyl)-dithieno[3,2-b:2',3'-d]thiophene) (PBPDT).

Using a procedure similar to that described above for **PBPT**, *(Z)*-1,2-bis(4-tert-butyl(phenyl))-1,2-bis(4,4,5,5-teramenthyl-1,3,2-dioxaborolan-2-yl)ethane (1.089 g, 2 mmol), 2,6-dibromodithieno[3,2-b:2',3'-d]thiophene (0.708 g，2 mmol) were polymerized to give **PBPDT**. The copolymer is a dark red powder finally. Yield: 0.728 g, (74.8 %).^{1}H NMR (400 MHz, CD_2Cl_2) δ: 7.39 – 7.29 (m, 4H), 7.29 – 6.87 (m, 4H), 6.61-6.30 (m, 2H), 1.37 – 0.84 (m, 18H); ^{13}C NMR (100 MHz, CD_2Cl_2) δ: 130.76, 129.13, 124.78, 123.06, 34.66, 31.18, 24.44. $C_{30}H_{28}S_3$ (484.74): C, 74.33; H, 5.82; S, 19.84. Found: C, 73.85; H, 6.38; S, 19.89 %.

Results and discussion

Synthesis and thermal characteristics

As shown in Scheme 1, the alternating copolymers were synthesized via Suzuki coupling by copolymerized *(Z)*-1,2-bis(4-tert-butyl(phenyl))-1,2-bis(4,4,5,5-teramenthyl-1,3,2-dioxaborolan-2-yl)ethane with 2,5-diiodothiophene，2,5-dibromothieno[3,2-b]thiophene and 2,6-dibromodithieno[3,2-b:2',3'-d]thiophene to prepare **PBPT**, **PBPTT** and **PBPDT** with the yields 44.3 %，66.1 % and 74.8 %, respectively. The monomer 2,5-dibromothiophene was replaced by 2,5-diiodothiophene, because the reaction activity of 2,5-dibromothiophene is not high enough to make a copolymer with high molecular weight. The molecular weight information of the three copolymers analyzed by GPC is summarized in Table 1 and Fig. S6†. The ^{1}H-NMR and ^{13}C-NMR spectra (Fig. S7-9†) prove the success of the polymerizations. Three copolymers have significant solubility in THF, chloroform, dichloromethane and some other solvent owing to the t-butyl side chains, which gives them the promising potential to be applied in a large scale solution process.

The thermal decomposition temperatures of these polymers were evaluated by TGA under a nitrogen atmosphere, as shown in Fig. S10-12†. The decomposition temperatures of **PBPT**, **PBPTT** and **PBPDT** are 388 °C, 330 °C and 351 °C, respectively. Differential scanning calorimetry (DSC) of the three copolymers shows no obvious thermal transition from 0 °C to 300 °C (Fig. S10-12†), probably because of the rigidity of the copolymer backbones.[43] The thermal tests indicate that all the copolymers have good thermal stability for OFET application.

Table 1 Physical and optical characteristics of **PBPT**, **PBPTT** and **PBPDT**

Compond	M_n[a] (kDa)	PDI[a]	Solution[b]			Film[c]		
			λ_{abs} (nm)	λ_{em} (nm)	E_g[d] (eV)	CVs		
						$E_{onset\text{-}ox}$[e] (V)	E_{HOMO}[f] (eV)	E_{LUMO}[g] (eV)
PBPT	24.7	1.3	405	612	2.30	0.43	-5.18	-2.88
PBPTT	7.8	1.1	494	618	2.13	0.39	-5.14	-3.01
PBPDT	13.6	1.4	485	618	2.16	0.33	-5.08	-2.92

[a] Determined by GPC (THF) against polystyrene. [b] Measurements performed in a dilute chloroform solution (10^{-5} M). [c] Measurements performed on a film from drop solution dry at room temperature. [d] Estimate from the cross point of UV-vis absorption and PL emission spectra (E_g=1240/$\lambda_{cross\text{-}point}$). [e] $E_{onset\text{-}ox}$ is the onset potential for oxidation. [f] Calculated using the empirical equation: E_{HOMO} = -($E_{onset\text{-}ox}$-0.0468+4.8) eV. [g] $E_{LUMO} = E_g + E_{HOMO}$

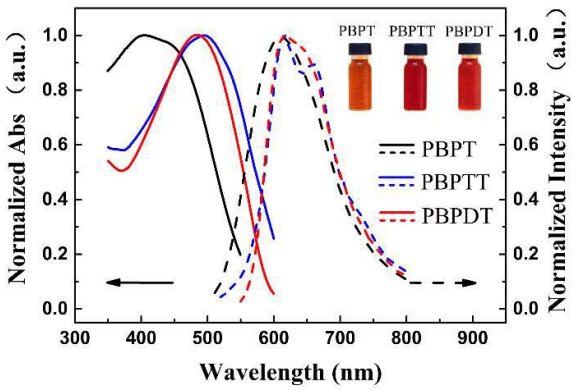

Fig. 1 Normalized UV-vis absorption and PL emission spectra of the copolymers in chloroform solution. The photos of **PBPT**, **PBPTT** and **PBPDT** solution are at the top right corner of the figure.

Optical and electrochemical characteristics

The UV-vis absorption and PL emission spectra of the copolymers in dilute chloroform solution (10^{-5} M) are shown in Fig. 1. Table 1 summarizes the optical data of the copolymers including the absorption peak wavelengths (λ_{abs}), emission peak wavelengths (λ_{em}) and optical band gaps (E_g). The absorption maxima of **PBPT**, **PBPTT** and **PBPDT** are at 405 nm, 494 nm and 485 nm respectively. The absorption peaks of **PBPDT** and **PBPTT** have apparent red shifts of 80nm and 89nm compared to that of **PBPT**. Additionally, in the long wave region, the PL emission spectra of **PBPTT** and **PBPDT** both have a shoulder peak which that of **PBPT** has not. It indicates that the fused thiophene obviously increases the molecular coplanarity and expends the intramolecular conjugated degree. What is more worth mentioning is that **PBPTT** has the most red-shifted absorption. It shows that the symmetric molecular structure of thieno[3,2-b]thiophene moiety makes polymer backbone a more planar conformation, probably like the "ribbon" shown in the Scheme 1.

Optical band gaps (E_g) are approximately derived from the crossing point of UV-vis absorption and PL emission spectra. The cross points of **PBPT**, **PBPTT**, **PBPDT** are at 538 nm, 582 nm and 574 nm respectively, corresponding to the optical band gaps of 2.30 eV, 2.13 eV and 2.16 eV. In accord with the result of the UV spectrum, **PBPTT** with thieno[3,2]thiophene shows the narrowest optical band gap, owing to its most planar molecular conformation. The data of E_{HOMO} and E_{LUMO} for the three copolymers were obtained by the cyclic voltammetry (Fig. S13†) and summarized in Table 1. The values of E_{HOMO} for **PBPT**, **PBPTT** and **PBPDT** all match well with the working function of gold (-5.1 eV) which will enhance the effective hole injection between the electrodes and semi-conductive copolymers, tending to promote the device performance.[43]

The orientation of aggregation structure and morphology

The orientation of polymer aggregation structure in the semiconductor layer is essential to OFET performance,[44-46]

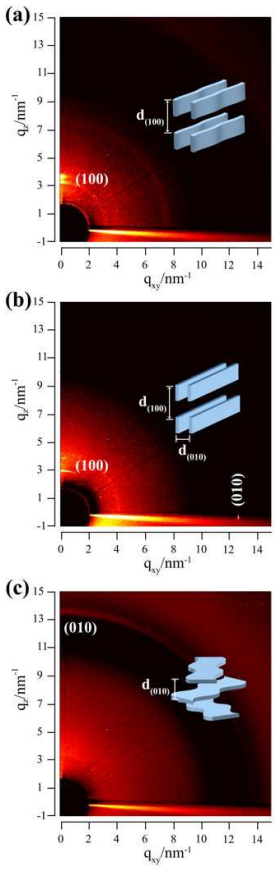

Fig. 2 The 2D GIXRD patterns of (a) **PBPT**, (b) **PBPTT** and (c) **PBPDT**. The insets in (a-c) are schematic diagrams of the orientations of the aggregation structure with respect to the substrate in the films.

because a charge-hopping transport mechanism dominates the charge carrier mobility in conjugated polymers.[47-49] Two dimensional grazing-incidence X-ray diffraction (2D GIXRD) was used to study the orientation structure of the 70-120 nm copolymer films which were spin-coated on substrates from 0.1 wt % chloroform at room temperature. There are mainly two kinds of reflections in the tree patterns, (100) reflections due to the lamellar layer structure and (010) reflection due to π-π intermolecular stacking.[50-52] In Fig. 2(a), **PBPT** shows a (100) reflection in the area of q_z = 3.1-3.8 nm^{-1} (out of plane). The d-spacing of this lamellar plane is 1.82 nm when the q_z is selected the average number 3.45 nm^{-1}. The (100) reflection only appears along the q_z axis, which indicates tert-butyl side-chains oriented with an edge-on structure on the substrate.[53, 54] The (010) reflection doesn't show on the pattern, probably due to the weak interlayer interaction caused by the poor coplanarity of the **PBPT** backbone, as shown in the inset of Fig. 2(a) schematically. It has been proved by UV spectra. The pattern of **PBPTT** (Fig. 2(b)) shows both (100) and (010) reflections along the q_z and q_{xy} (in plane) axis, identifying the

edge-on chain conformation to the substrate. This result indicates the (100) axis is normal to the substrate and the (010) axis parallel to the plane of the substrate, as shown in the inset of Fig. 2(b). The (100) reflection is at q_z =2.9-3.9 nm^{-1}. The d-spacing of these (100) planes is 1.85 nm derived by the average number of q_z. The d-spacing of the (010) plane is 0.49 nm as q_{xy} = 12.7 nm^{-1}. The lamellar layer d-spacing of **PBPTT** is larger than that of **PBPT**, probably because the thieno[3,2-b]thiophene moiety is wider than thiophene moiety. The **PBPDT** film only shows (010) reflection (q_z =13.6 nm^{-1} d-spacing=0.46 nm^{-1}) along q_z, indicating the π-π stacking planes is parallel to the substrate in the face-on way,[53, 54] as shown in Fig. 2(c). The d-spacing of **PBPDT** is a little narrower than that of **PBPTT** probably owing to the stronger π-π stacking effect from the bigger conjugated structure of dithieno[3,2-b:2',3'-d]thiophene . The absence of (100) reflection is probably due to the twist of polymer conformation caused by the asymmetry of the dithieno[3,2-b:2',3'-d]thiophene moiety, as shown in the inset of Fig. 2(c). In addition, although the thiophene and dithieno[3,2-b:2',3'-d]thiophene both are asymmetrical，there is (100) diffraction reflection in the **PBPT** sample. It can be explained by that the steric hindrance of thiophene moiety is relatively smaller than that of fused thiophene, so the molecular chain can stack in partially ordered packing structure through the rotation of the thiophene ring.

In summary, the 2D GIXRD results demonstrate the copolymer with thieno[3,2-b]thiophene moiety has both the lamellar structure and π-π stacking in the thin film, probably indicating that the symmetric structure of thieno[3,2-b]thiophene can induce a straight "ribbon-like" molecular conformation in aggregation state.

AFM is used to observe the microscopic morphology of the three copolymer thin films, as shown in Fig. 3(a-c). The **PBPT** and **PBPDT** films do not show the obvious ordered structure, but exit some granules which may be formed by the aggregation effect of the copolymers. Compared with the **PBPT** film, the **PBPDT** has a rougher surface, which can be explained by the stronger aggregation caused by the dithieno[3,2-b:2',3'-d]thiophene moiety. In contrast, we can clearly observe fiber-like structures of **PBPTT** film in Fig. 3(b). These fibers are approximately 1 μm long and 20 nm wide. Another bigger AFM photo (5 μm×5 μm) of **PBPTT** shows that this copolymer film forms uniform fiber-like morphology at a very large scale (Fig. S14†). Further, polarizing microscope (POM) was also used to study the copolymer morphology. The samples were precipitated from the chloroform solution of three copolymers at room temperature. **PBPDT** and **PBPT** didn't show the obvious regular structures in bright field (Fig. S15†) and had no birefringence phenomena. In contrast, a lot of ordered aggregation structures (about 20 μm length) were observed in the sample of **PBPTT**, as shown in Fig. 3(d) and Fig. S15†. The strong birefringence under the cross polarized light indicates **PBPTT** has an instructive ability to form highly ordered packing structure in the solid state.

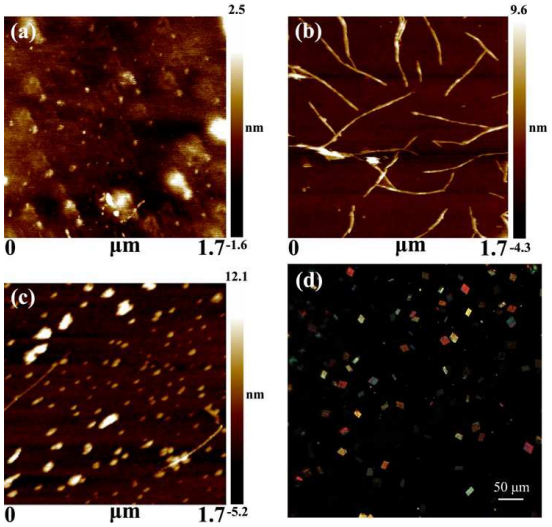

Fig. 3 AFM images of (a) **PBPT**, (b) **PBPTT** and (c) **PBPDT** films on 1.7μm×1.7 μm. (d) POM photo of **PBPTT** under cross polarized light.

The AFM and POM photos show **PBPTT** has greater ability to form regular morphology in the film than **PBPT** and **PBPDT**. Such fiber-like film morphology can be expected to give better charge-carrier mobility as well as ambient stability for OFET devices.

OFET Device performance

As Fig. 4 (a) shown, the top-gate and bottom contact OFET devices based on **PBPT**, **PBPTT** and **PBPDT** were fabricated on the PET substrates, with Au source/drain electrodes and ion gel as the dielectric layers. They can be easily bent by hand force.

The transfer plots (Fig. 4(b)-(d)) and output curves (Fig. S16†) of the devices exhibited typical p-channel OFET characteristics. Charge carrier mobility and threshold voltage are obtained from the fitting (red dashed line) of the transfer plot data at the saturation regime according the following equation:

$$I_{DS} = (\mu W C_i / 2L) (V_G - V_{TH})^2$$

PBPTT has the best OFET performance with a very small threshold voltage of -0.13 V, which is consistent with the results of band gaps, aggregation structure and morphology characterizations. The mobility of **PBPDT** is better than **PBPT**. It indicates the charge carrier mobility of copolymer has a better correlation with the π-π interchain transport.[50]

A test was done to research the **PBPTT** OFET devices performance when it underwent bend towards two opposite directions, as shown in Fig.5 (a) (d). The device in the most middle of the array was tested, to ensure it is undergoing the most intensive bending. In addition, the device was the same one that tested in the flat condition (Fig. 4 (c)), which can assure the comparability of the data gotten from these three conditions.

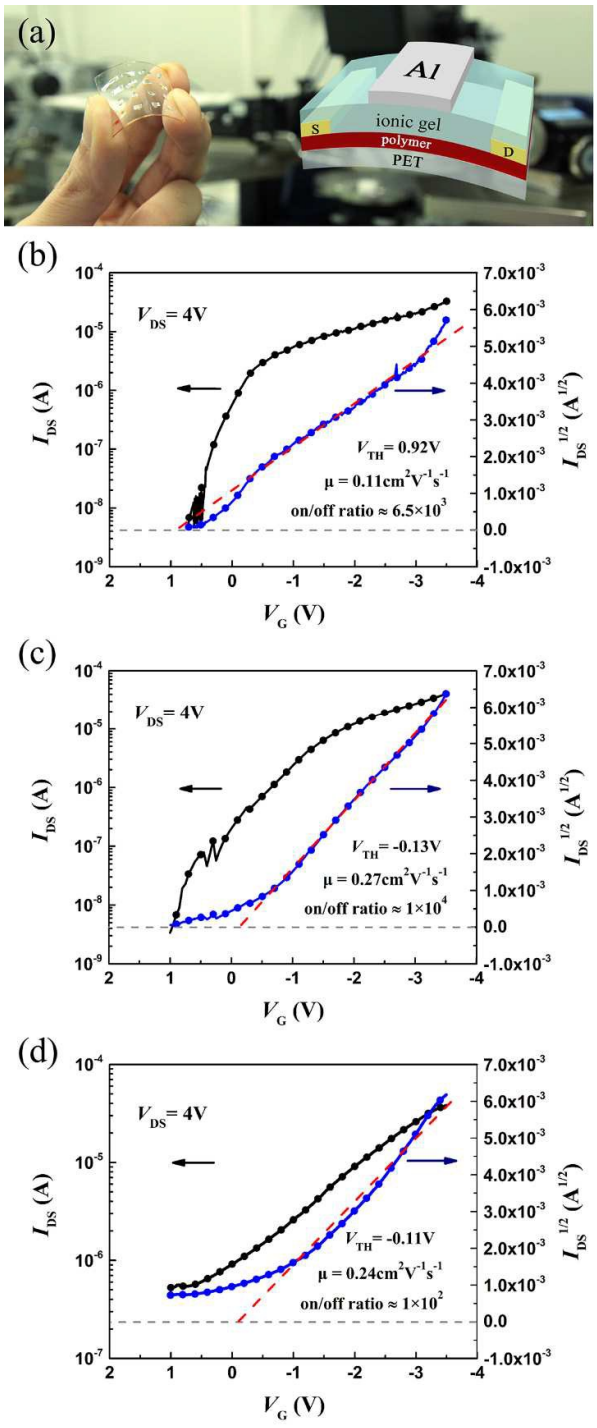

Fig. 4 (a) The photo and schematic structure of the flexible OFET device based on ionic gel dielectric layer. The transfer plots of the OFET devices based on (b)**PBPT**, (c)**PBPTT**, (d)**PBPDT**

The transfer plots (Fig. 5 (b) (e)) show the charge carrier mobility of the device was 0.25 $cm^2V^{-1}s^{-1}$ and 0.24 $cm^2V^{-1}s^{-1}$ under the two different bending conditions. They are only a little lower than the mobility in the flat condition. As shown in Fig. 5 (c) (f), all the curves are through the origins in the output plots, it means there are not any electric leakage phenomena of the device under bending. In general, the bent OFET device maintains its great performance.

This ability to keep great performance through deformation probably owes to the merits of the ion gel dielectric layers. The interface between the semi-conductor layer and dielectric layer has decisive influence on the performance of the device，because charge carriers accumulate and translate at this interface.[55, 56] If the semiconductor layer was detached from the insulting layer when the device was bent, the device performance will decrease greatly. The ion gel layer in this device has great flexibility and adhesiveness to the organic semiconductor layer, so it ensures the intimate contact of the two layers under intensive deformation.

Another major issue for OFET is the poor ambient stability of the organic semiconductor polymer, which mainly comes from the influence of O_2 and H_2O in the air. [55, 57-59] We stored the **PBPTT** devices in the environment of 30 °C and the humidity 50 % for two weeks. The OFET characteristics were tested every two days on the same device (Fig. S18†). Its charge carrier mobility, on/off ratio and threshold voltage are all summarized in Table S2†. The charge carrier mobilities of the **PBPTT** OFET never decrease in the test during two weeks. The on/off ratios decline a little, but it remains more than 1×10^3. The great ambient stability can owe to the ordered aggregation structure of **PBPTT** and the presence of the encapsulation effect of the ion gel dielectric layer. These two factors make the **PBPTT** OFET device can resist the break-in of O_2 and H_2O in the humid condition.

Conclusions

In this study, three polymers were synthesized by copolymerization of *(Z)*-1,2-bis(4-(tert-butyl)phenyl)ethane with thiophene, thieno[3,2-b]thiophene and dithieno[3,2-b:2',3'-d]thiophene respectively. The influence of different thiophene comonomers on the copolymer optical properties, aggregation structure, film morphology and device performance were investigated. It is found that the symmetric chemical structure of thieno[3,2-b]thiophene and cis configuration of *(Z)*-1,2-bis(4-(tert-butyl)phenyl)ethane make **PBPTT** the almost coplanar conformation in molecular level, which proves the success of our synthetic strategy. The 2D GIXRD results show **PBPTT** has the most ordered aggregation structure in edge-on orientation with respect to the substrate. The AFM and POM photos show **PBPTT** owning fiber-like morphology of the spin-coating film and lamellar aggregation structure of the precipitate. The OFET devices were fabricated based on **PBPT**, **PBPTT** and **PBPDT**, with the charge carrier mobilities up to 0.11, 0.27 and 0.24 $cm^2V^{-1}s^{-1}$,respectively. The **PBPTT** OFET devices show the best performance, with the on/off ratio of 10^4 and a very low threshold voltage of -0.13 V. In addition, the bending and ambient stability tests were carried on the devices of **PBPTT.** The polymer ordered

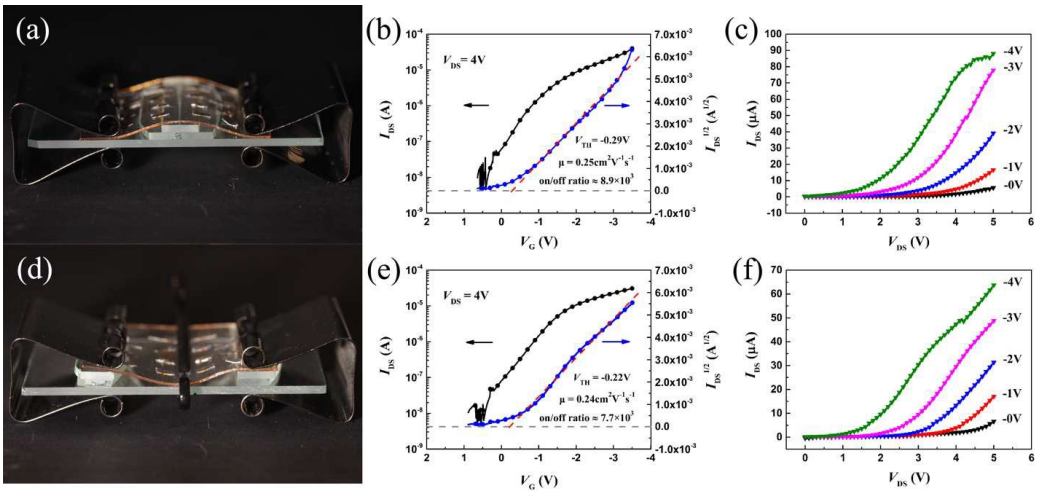

Fig. 5 The photos of bended OFET device during the test(a, d). The transfer plots (b, e) and typical output curves (c, f) of the OFET device base on **PBPTT**

aggregation structure and encapsulation effect of ion gel provide a good resistance to O_2 and H_2O. The flexible and adhesive ion gel dielectric layers maintain the great performance of the devices under deformation. In summary, such ambient stable, flexible OFET devices have a bright prospect in the application, owing to the good solubility and ordered aggregation structure of **PBPTT** with the flexibility, adhesiveness and encapsulation effect of ion-gel dielectric layer.

Acknowledgements

This work was financially supported by the National Natural Science Foundation of China (21274027 and 20974022) and the Innovation Program of Shanghai Municipal Education Commission (15ZZ002). The synchrotron-based 2D-GIXRD measurement was supported by Shanghai Synchrotron Radiation Facility (15ssrf00474). The OFET devices were fabricated and probed in the nanofab of Fudan university.

Notes and references

1. Y. Diao, B. C. Tee, G. Giri, J. Xu, H. Kim do, H. A. Becerril, R. M. Stoltenberg, T. H. Lee, G. Xue, S. C. Mannsfeld and Z. Bao, *Nat. Mater.*, 2013, **12**, 665-671.
2. H. Liu, C. H. Reccius and H. G. Craighead, *Appl. Phys. Lett.*, 2005, **87**, 253106.
3. H. Minemawari, T. Yamada, H. Matsui, J. Tsutsumi, S. Haas, R. Chiba, R. Kumai and T. Hasegawa, *Nature*, 2011, **475**, 364-367.
4. Y. D. Park, H. S. Lee, Y. J. Choi, D. Kwak, J. H. Cho, S. Lee and K. Cho, *Adv. Funct. Mater.*, 2009, **19**, 1200-1206.
5. L. Qiu, W. H. Lee, X. Wang, J. S. Kim, J. A. Lim, D. Kwak, S. Lee and K. Cho, *Adv. Mater.*, 2009, **21**, 1349-1353.
6. H. Bronstein, Z. Chen, R. S. Ashraf, W. Zhang, J. Du, J. R. Durrant, P. S. Tuladhar, K. Song, S. E. Watkins, Y. Geerts, M. M. Wienk, R. A. Janssen, T. Anthopoulos, H. Sirringhaus, M. Heeney and I. McCulloch, *J. Am. Chem. Soc.*, 2011, **133**, 3272-3275.
7. A. Facchetti, *Materials Today*, 2007, **10**, 28-37.
8. B. A. Jones, A. Facchetti, M. R. Wasielewski and T. J. Marks, *J. Am. Chem. Soc.*, 2007, **129**, 15259-15278.
9. M. M. Ling and Z. Bao, *Chem. Mater.*, 2004, **16**, 4824-4840.
10. J. Mei, Y. Diao, A. L. Appleton, L. Fang and Z. Bao, *J. Am. Chem. Soc.*, 2013, **135**, 6724-6746.
11. M. Halik, H. Klauk, U. Zschieschang, T. Kriem, G. n. Schmid, W. Radlik and K. Wussow, *Appl. Phys. Lett.*, 2002, **81**, 289.
12. J. Veres, S. Ogier, G. Lloyd and D. de Leeuw, *Chem. Mater.*, 2004, **16**, 4543-4555.
13. A. L. Briseno, R. J. Tseng, M. M. Ling, E. H. L. Falcao, Y. Yang, F. Wudl and Z. Bao, *Adv. Mater.*, 2006, **18**, 2320-2324.
14. M. A. Reyes-Martinez, A. J. Crosby and A. L. Briseno, *Nat. Commun.*, 2015, **6**, 6948.
15. T. Sekitani, Y. Kato, S. Iba, H. Shinaoka, T. Someya, T. Sakurai and S. Takagi, *Appl. Phys. Lett.*, 2005, **86**, 073511.
16. J. Lee, M. J. Panzer, Y. He, *J. Am. Chem. Soc.*, 2007, **129**, 4532-4533.
17. J. H. Cho, J. Lee, Y. He, B. S. Kim, T. P. Lodge and C. D. Frisbie, *Adv. Mater.*, 2008, **20**, 686-690.
18. J. H. Cho, J. Lee, Y. Xia, B. Kim, Y. He, M. J. Renn, T. P. Lodge and C. D. Frisbie, *Nat. Mater.*, 2008, **7**, 900-906.
19. T. Fujimoto and K. Awaga, *Phys. Chem. Chem. Phys.*, 2013, **15**, 8983-9006.
20. M. Ha, Y. Xia, A. A. Green, W. Zhang, M. J. Renn, C. H. Kim, M. C. Hersam and C. D. Frisbie, *ACS Nano*, 2010, **4**, 4388-4395.
21. Y. He, P. G. Boswell, P. Buhlmann and T. P. Lodge, *J. Phys. Chem. B*, 2007, **111**, 4645-4652.
22. R. Horita, K. Ohtani, T. Kai, Y. Murao, H. Nishida, T. Toya, K. Seo, M. Sakai and T. Okuda, *Jap. J. Appl. Phys.*, 2013, **52**, 115803.
23. T. Ueki and M. Watanabe, *Macromolecules*, 2008, **41**, 3739-3749.
24. S. W. Lee, H. J. Lee, J. H. Choi, W. G. Koh, J. M. Myoung, J. H. Hur, J. J. Park, J. H. Cho and U. Jeong, *Nano Lett.*, 2010, **10**, 347-351.

25. M. A. Susan, T. Kaneko, A. Noda and M. Watanabe, *J. Am. Chem. Soc.*, 2005, **127**, 4976-4983.
26. Z. Bao, A. Dodabalapur and A. J. Lovinger, *Appl. Phys. Lett.*, 1996, **69**, 4108.
27. J. E. Donaghey, E.-H. Sohn, R. S. Ashraf, T. D. Anthopoulos, S. E. Watkins, K. Song, C. K. Williams and I. McCulloch, *Poly. Chem.*, 2013, **4**, 3537.
28. Y. Li, Y. Wu, P. Liu, M. Birau, H. Pan and B. S. Ong, *Adv Mater.*, 2006, **18**, 3029-3032.
29. I. McCulloch, M. Heeney, C. Bailey, K. Genevicius, I. Macdonald, M. Shkunov, D. Sparrowe, S. Tierney, R. Wagner, W. Zhang, M. L. Chabinyc, R. J. Kline, M. D. McGehee and M. F. Toney, *Nat. Mater.*, 2006, **5**, 328-333.
30. S. Zou, Y. Wang, J. Gao, X. Liu, W. Hao, H. Zhang, H. Zhang, H. Xie, C. Yang, H. Li and W. Hu, *J. Mater. Chem. C*, 2014, **2**, 10011-10016.
31. H. Sirringhaus, *Science*, 1998, **280**, 1741-1744.
32. K.-J. Baeg, D. Khim, D.-Y. Kim, J. B. Koo, I.-K. You, W. S. Choi and Y.-Y. Noh, *Thin Solid Films*, 2010, **518**, 4024-4029.
33. R. Li, H. Dong, X. Zhan, H. Li, S.-H. Wen, W.-Q. Deng, K.-L. Han and W. Hu, *J. Mater. Chem.*, 2011, **21**, 11335.
34. Y. Liu, Y. Liu and X. Zhan, *Macromol. Chem. Phys.*, 2011, **212**, 428-443.
35. I. Meager, M. Nikolka, B. C. Schroeder, C. B. Nielsen, M. Planells, H. Bronstein, J. W. Rumer, D. I. James, R. S. Ashraf, A. Sadhanala, P. Hayoz, J.-C. Flores, H. Sirringhaus and I. McCulloch, *Adv. Funct. Mater.*, 2014, 2014, **24**, 7109-7115
36. C. Niebel, Y. Kim, C. Ruzié, J. Karpinska, B. Chattopadhyay, G. Schweicher, A. Richard, V. Lemaur, Y. Olivier, J. Cornil, A. R. Kennedy, Y. Diao, W.-Y. Lee, S. Mannsfeld, Z. Bao and Y. H. Geerts, *J. Mater. Chem. C*, 2015, **3**, 674-685.
37. K. Takimiya, I. Osaka, T. Mori and M. Nakano, *Acc. Chem. Res.*, 2014, **47**, 1493-1502.
38. W. Wu, Y. Liu and D. Zhu, *Chem. Soc. Rev.*, 2010, **39**, 1489-1502.
39. S. Zhang, Y. Guo, Y. Zhang, R. Liu, Q. Li, X. Zhan, Y. Liu and W. Hu, *Chem. Commun.*, 2010, **46**, 2841-2843.
40. J.W. Yang, Y.L. Huang and W.Z. Wang, *J. Mater. Chem. C*, 2015, **3**, 10074-10078
41. W.-Q. Deng and W. A. Goddard, *J. Phys. Chem. B*, 2004, **108**, 8614-8621.
42. S. H. Wen, A. Li, J. Song, W. Q. Deng, K. L. Han and W. A. Goddard, *J. Phys. Chem. B*, 2009, **113**, 8813-8819.
43. K. Lu, C.-a. Di, H. Xi, Y. Liu, G. Yu, W. Qiu, H. Zhang, X. Gao, Y. Liu, T. Qi, C. Du and D. Zhu, *J. Mater. Chem.*, 2008, **18**, 3426.
44. R. Joseph Kline, M. D. McGehee and M. F. Toney, *Nat. Mater.*, 2006, **5**, 222-228.
45. Y. Kim, S. Cook, S. M. Tuladhar, S. A. Choulis, J. Nelson, J. R. Durrant, D. D. C. Bradley, M. Giles, I. McCulloch, C.-S. Ha and M. Ree, *Nat. Mater.*, 2006, **5**, 197-203.
46. G. Li, Y. Yao, H. Yang, V. Shrotriya, G. Yang and Y. Yang, *Advanced Functional Materials*, 2007, **17**, 1636-1644.
47. Z. H. Chen, P. Muller and T. M. Swager, *Org. Lett.*, 2006, **8**, 273-276.
48. S. R. Forrest, *Chem. Rev.*, 1997, **97**, 1793-1896.
49. A. Salleo, R. J. Kline, D. M. DeLongchamp and M. L. Chabinyc, *Adv. Mater.*, 2010, **22**, 3812-3838.
50. S. R. Forrest, *Chem. Rev.*, 1997, **97**, 1793-1896.
51. K. E. Aasmundtveit, E. J. Samuelsen, M. Guldstein, C. Steinsland, O. Flornes, C. Fagermo, T. M. Seeberg, L. A. A. Pettersson, O. Inganas, R. Feidenhans'l and S. Ferrer, *Macromolecules*, 2000, **33**, 3120-3127.
52. R. Kim, P. S. K. Amegadze, I. Kang, H.-J. Yun, Y.-Y. Noh, S.-K. Kwon and Y.-H. Kim, *Adv. Funct. Mater.*, 2013, **23**, 5719-5727.
53. Y. Qu, Q. Su, S. Li, G. Lu, X. Zhou, J. Zhang, Z. Chen and X. Yang, *ACS Macro. Lett.*, 2012, **1**, 1274-1278.
54. S. Shao, J. Liu, J. Zhang, B. Zhang, Z. Xie, Y. Geng and L. Wang, *ACS Appl. Mater. Inter.*, 2012, **4**, 5704-5710.
55. H. Dong, L. Jiang and W. Hu, *Phys. Chem. Chem. Phys.*, 2012, **14**, 14165-14180.
56. H. Ma, H.-L. Yip, F. Huang and A. K. Y. Jen, *Adv. Funct. Mater.*, 2010, **20**, 1371-1388.
57. H.-S. Kim, Y.-H. Kim, T.-H. Kim, Y.-Y. Noh, S. Pyo, M. H. Yi, D.-Y. Kim and S.-K. Kwon, *Chem. Mater.*, 2007, **19**, 3561-3567.
58. H. Pan, Y. Li, Y. Wu, P. Liu, B. S. Ong, S. Zhu and G. Xu, *J. Am. Chem. Soc.*, 2007, **129**, 4112-4113.
59. K. Schmoltner, F. Schlütter, M. Kivala, M. Baumgarten, S. Winkler, R. Trattnig, N. Koch, A. Klug, E. J. W. List and K. Müllen, *Poly. Chem.*, 2013, **4**, 5337.

.

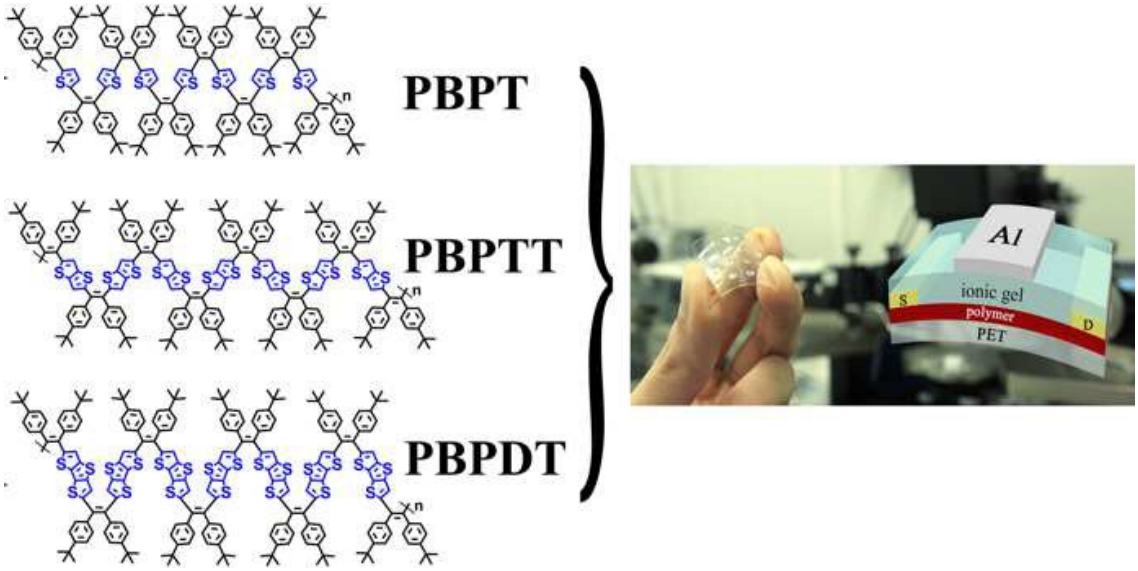

Three (*Z*)-1,2-bis(4-(tert-butyl)phenyl)ethane based copolymers were synthesized, and applied in the high performance flexible OFET devices.